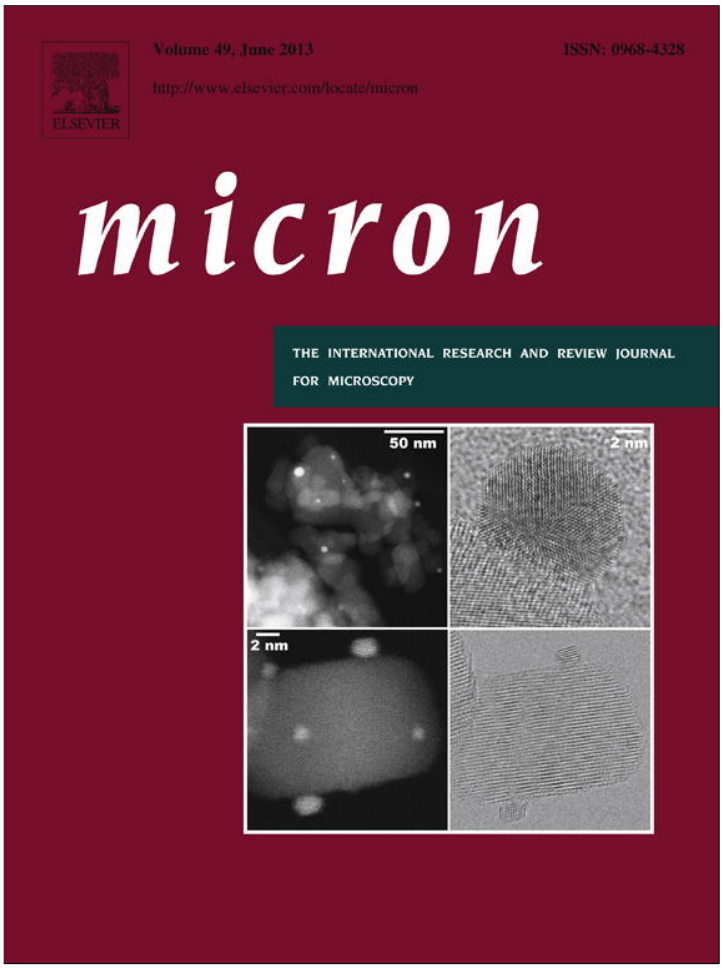

Micron 49 (2013) 21–27

Contents lists available at SciVerse ScienceDirect

Micron

journal homepage: www.elsevier.com/locate/micron

Morphology and thermal properties of clay/PMMA nanocomposites obtained by miniemulsion polymerization

Karla I. García-Chávez[a], Claudia A. Hernández-Escobar[a], Sergio G. Flores-Gallardo[a], Florentino Soriano-Corral[b], Esmeralda Saucedo-Salazar[b], E. Armando Zaragoza-Contreras[a,*]

[a] Centro de Investigación en Materiales Avanzados, S.C. Miguel de Cervantes No. 120, CP 31109, Chihuahua, Chih., Mexico
[b] Centro de Investigación en Química Aplicada, Blvd. Enrique Reyna No. 140, CP 25250, Saltillo, Coahuila, Mexico

ARTICLE INFO

Article history:
Received 1 February 2012
Received in revised form 27 February 2013
Accepted 27 February 2013

Keywords:
Clay polymer nanocomposites
Miniemulsion polymerization
Nanocomposite

ABSTRACT

Miniemulsion polymerization was used as the synthetic method to produce clay/poly(methyl methacrylate) nanocomposites. Two kinds of interfacial interactions clay–polymer particle were observed by electron microscopy, one where the polymer particles are adhered on the surface of the larger fragments of clay, and another where nanometric fragments of clay are encapsulated by polymer particles. Variations in the glass transition temperature (T_g) and thermomechanical properties of the matrix, as function of clay content, were observed. In particular, at the highest clay loading (1.0 wt%) depression of T_g and thermomechanical properties were observed. The increased clay–polymer matrix interfacial area appears to be the conditioning factor that determines such behavior.

1. Introduction

Clays comprise a group of materials with high impact on polymer composite research. Polymer–clay nanocomposites (PCNs) are by themselves a new class of organic–inorganic hybrid materials. PCNs present a wide variety of advantages and properties, for instance, improved modulus and strength, high heat distortion temperature, high specific stiffness, good thermal stability, and reduced gas permeability at low filler concentrations (Lu and Mai, 2005; Hao et al., 2005; Xu et a., 2006).

Emulsion polymerization techniques have demonstrated to be an appropriate strategy for the incorporation of clays into a wide range of polymer matrices, as reported in literature. Noh and Lee (1999) prepared sodium montmorillonite (MMT)/polystyrene nanocomposites by conventional emulsion polymerization. They suggested that the enhanced thermal and mechanical properties are attributed to the fixation of polymer chains into the interlayer of MMT and the restricted segmental motion near the organic–inorganic interfaces. They also suggested that the inorganic materials accumulate heat enough to transfer the glass transition upward. Xu et al. (2003) reported the synthesis and characterization of exfoliated styrene–acrylic copolymer/sodium montmorillonite nanocomposites by emulsion polymerization using an acrylamido-surfmer to stabilize the emulsion. The surfmer facilitated co-monomer diffusion into the clay platelets. Improvements in the mechanical properties as function of clay concentration were observed. Sun et al. (2004a,b) reported the encapsulation of laponite by polystyrene via miniemulsion polymerization. They found a complete exfoliation of the clay and concluded that clay hydrophobicity was determining in encapsulation and latex stability. Yeh et al. (2004) prepared poly(methyl methacrylate)/montmorillonite nanocomposites by in situ emulsion polymerization and by solution-dispersion polymerization. They found a much a better dispersion of the clay platelets into the polymer matrix by the emulsion polymerization with respect to the other method. Relevant literature can also be consulted (Lai et al., 2007; Negrete-Herrera et al., 2006a,b; Bouanani et al., 2008; Mirzataheri et al., 2009).

In the present study, a commercial nanoclay was used to modify poly(methyl methacrylate) (PMMA) using miniemulsion polymerization as the synthetic method. By this technique, a wide variety of nanomaterials has been encapsulated in polymer particles by taking advantage of the intrinsic nature of this method. The goal of this work was to achieve nanocomposites with improved physical properties at low filler concentrations based on the homogeneous dispersion of the clay in the matrix favored by the method of synthesis. Electron microscopy was a fundamental tool to give evidence of composite behavior.

* Corresponding author. Tel.: +52 614 139 4811; fax: +52 614 439 1130.
E-mail address: armando.zaragoza@cimav.edu.mx (E.A. Zaragoza-Contreras).

0968-4328/$ – see front matter © 2013 Elsevier Ltd. All rights reserved.
http://dx.doi.org/10.1016/j.micron.2013.02.007

2. Experimental

2.1. Materials

Commercial clay, Nanofil SE3000 (layered silicate based on a natural bentonite, modified with a dimethyl, di(hydrogenated tallow)alkyl ammonium salt), with average particle size of 6–8 μm, surface-area of 700 $m^2\,g^{-1}$, and apparent density of 450 $kg\,m^{-3}$ (Süd-Chemie AG, Clariant Group Co.) was used as the reinforcing material. Methyl methacrylate (MMA) (Aldrich Co.) was distilled under vacuum and kept under refrigeration. 2,2′-Azobisisobutironitrile (AIBN) (Aldrich Co.) was recrystalized from a saturated aqueous solution and kept at 5 °C until its usage. Sodium dodecylsulfate (Aldrich Co.) and hexadecane (Aldrich Co.) were used as delivered.

2.2. Nanocomposite synthesis

Clay/PMMA nanocomposites were synthesized as follows: first, sodium dodecylsulfate (SDS) (9.5 mmol L^{-1}) and tridistilled water (80 g) were loaded to a glass flask, and left for 15 min to allow SDS to stabilize in the water. Next, Nanofil SE3000 (0.125 wt%, 0.5 wt%, or 1.0 wt% with respect to PMMA content), hexadecane (0.83 g), and MMA (20 g) were loaded in a separate vessel. This mixture was sonicated for 15 min using an ultrasonic cleaner (model 2510, BRANSON). Afterwards, the clay dispersion was transferred to the water–surfactant solution to complete the system. To obtain a stable miniemulsion 45 min of sonication are required. Finally, AIBN (0.1 g) was fed to the miniemulsion 5 min before completing the sonication period. Once the miniemulsion was stabilized, the reactor was immersed in a bath tempered at 65 °C. This moment was considered as the beginning of the polymerization since the initiator was already in the system. Pure PMMA latex was obtained under the same condition for comparison purposes. Polymerization additional conditions were 300 rpm of mechanical agitation, nitrogen atmosphere, and 120 min of polymerization.

2.3. Characterization

2.3.1. Electron microscopy

The morphology of both clay and clay/PMMA composites (as obtained from the reactor) was studied using a field emission electron microscope (JSM-7401F, Jeol) with STEM mode. To prepare the samples, two drops of the composite latexes were diluted in 30 mL of distilled water and then dispersed for 5 min by sonication. Afterwards, a drop of the dispersion was placed on a holey carbon cooper grid. The energy dispersive X-ray analyzer (INCA Penta FETx3 EDX, Oxford Instruments) coupled to the microscope, was used to determine clay presence in the composite. Complementarily, clay distribution in the composites processed by compression molding was analyzed with a transmission electron microscope (G2 80-300 TEM, Titan). For this study, slices of 80 nm width were obtained using a cryogenic ultramicrotome (EM UC7, Leica); the samples were cut at −130 °C at a rate of 1.4 mm min^{-1}.

2.3.2. Thermal and mechanical properties

Nanocomposites glass transition temperature (T_g) was evaluated using a differential scanning calorimeter (Thermal Analyst 2100, TA Instruments). The thermograms were obtained firstly heating the sample from ambient to 180 °C, to eliminate thermal effects fixed during the synthesis, then cooled to 30 °C and heated again to 250 °C. The T_g was taken from the second heating process. The samples were run in air atmosphere at a heating rate of 10 °C min^{-1}. A sample of pure PMMA was analyzed as reference. Additionally, the composites were characterized using a mechanical dynamical analyzer (RSA III DMA, TA Instruments). Probes of 5 cm × 1 cm × 0.2 mm, of pure PMMA and the composites, were prepared by compression molding at 250 °C. Sweep temperature from 40 °C to 200 °C, fixed frequency of 1 Hz, and strain of 0.1 mm were the analysis conditions.

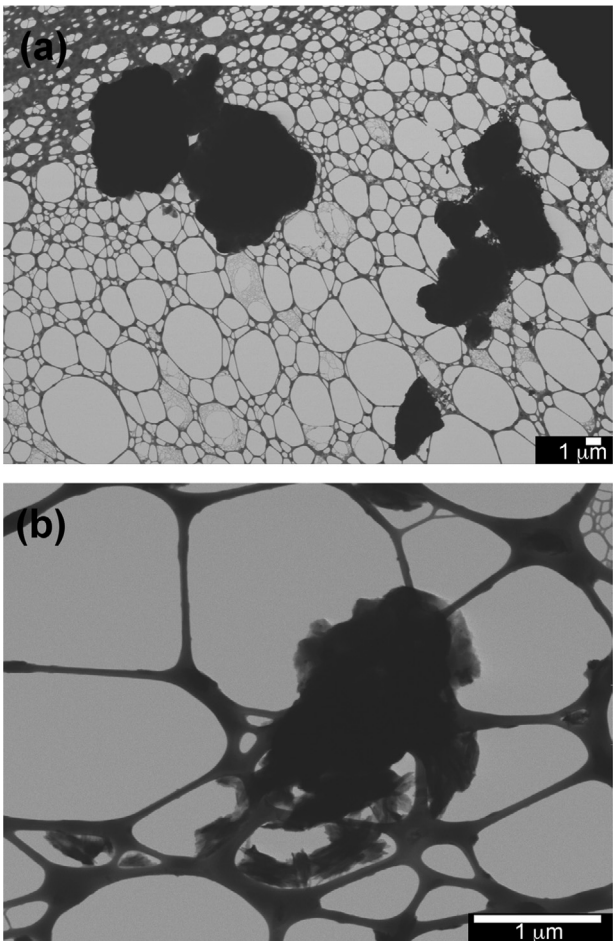

Fig. 1. Micrographs of pristine Nanofill SE3000. Two kinds of clay particles are observed. (a) Micrometric particles and (b) submicrometric particles.

3. Results and discussion

3.1. Composite synthesis

Miniemulsion polymerizations were performed using SDS slightly above its critical micellar concentration (cmc) (8.0 mmol L^{-1} at 25 °C). Since the polymerizations were run under heating (65 °C), the increment in the temperature produces modification of the cmc causing latex instability (clay presence must also be considered). Thus, miniemulsion polymerizations were performed in the presence of 1.0 wt% clay, increasing SDS concentration progressively until no solid precipitation was observed. This way, stable latexes were obtained at 9.5 mmol L^{-1} of SDS. It is worth commenting that AIBN (a monomer soluble initiator) was used as the initiator to favor droplet nucleation.

3.2. Composite morphology

Fig. 1(a and b) portraits microscopy images of the pristine clay. As noted, clay comprises two kinds of particles, a group of large solid particles in the order of 1 to several microns, and a much more abundant group of elongated particles, smaller than 500 nm. In the case of the composites, microscopy showed that the large solid

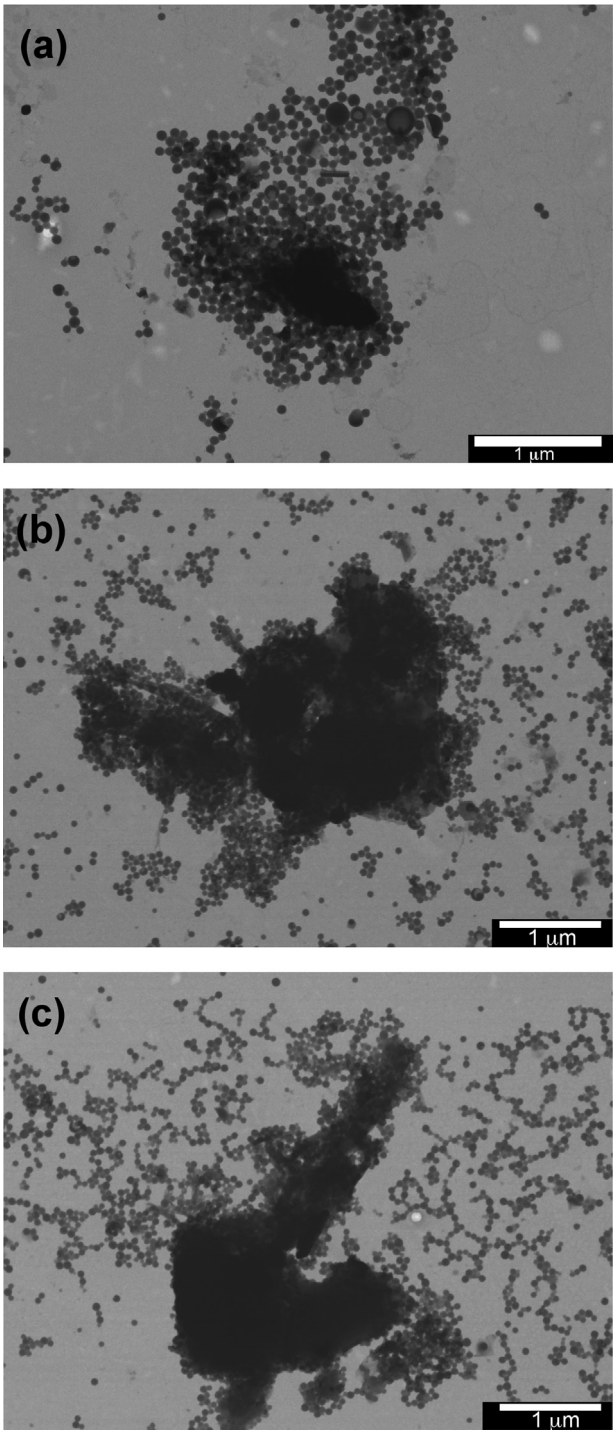

Fig. 2. Micrographs of the clay/PMMA nanocomposites obtained by miniemulsion polymerization. (a) 0.125 wt%, (b) 0.5 wt% and (c) 1.0 wt%. Polymer particles are adhered on the surface of micrometric clay fragments.

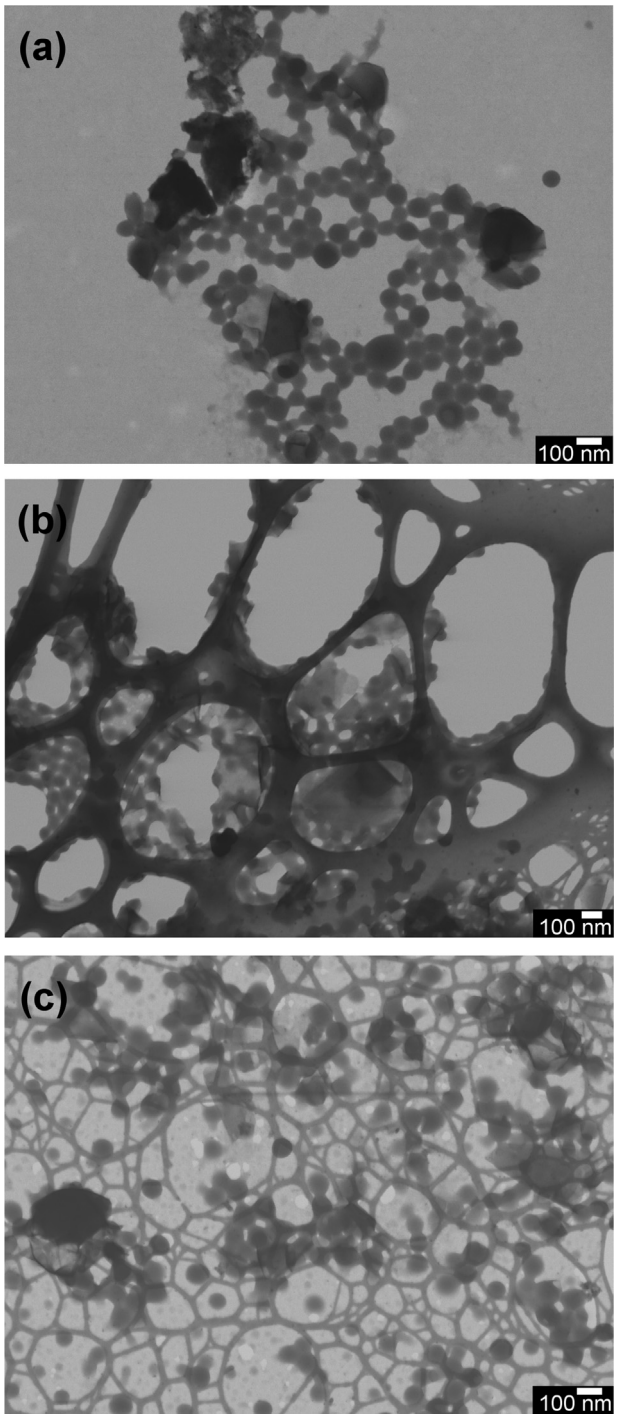

Fig. 3. Micrographs of the clay/PMMA nanocomposites obtained by miniemulsion polymerization. (a) 0.125 wt%, (b) 0.5 wt% and (c) 1.0 wt%. Fragments of submicrometric size show clay fragmentation.

particles fragmented in a wide range of particle sizes. Fig. 2(a–c) portraits micrographs of the composites where micrometric fragments of clay are present; whereas in Fig. 3(a–c) fragmentation of this particles to submicrometric size are evident. As noted in the series of images, the clay fragments are too big with respect to the PMMA particles (<100 nm), which in first instance denoted that encapsulation is not possible, considering clay dimensions. However, the affinity between the PMMA particles and the clay is evident since the polymer particles appear to be adhered on the clay surface, especially on the larger fragments.

It is worth noting that during composite analysis by microscopy, a significant amount of polymer particles with larger diameters (>100 nm) and different appearance (clear core and deformation) were observed. Fig. 4 portraits a micrograph where those particles are clearly observed. Tong and Deng (2007) found, during the encapsulation of nanosaponite (50 nm) into polystyrene host that the latex was comprised of two main groups of particles: spherical particles with a size less than 100 nm and hemispherical or bowl-structured particle with size in the range 100–1000 nm. They performed EDX analysis on these particles and found evidence of

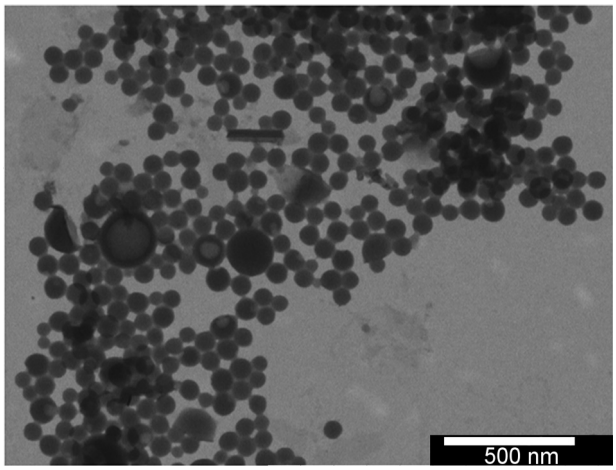

Fig. 4. Micrographs of the hemispherical or bowl-structured particle.

silicon within them even though the saponite was not seen from the latex surface, which suggested saponite encapsulation by polymer particles. Taking into account the similarity of the bowl-structured particles reported by Tong and Deng, and the particles found in this study, EDX analysis was also performed. Fig. 5 portraits the EDX analysis performed on the sample of the composite containing 1.0 wt% clay. As seen, the spectrum indicated the presence of silicon in the area of analysis, which indicates that a clay fragment was encapsulated by the polymer particle. Consequently, because of the size of the smaller clay particles observed in Fig. 1, we consider that these have the appropriate dimension to be encapsulated

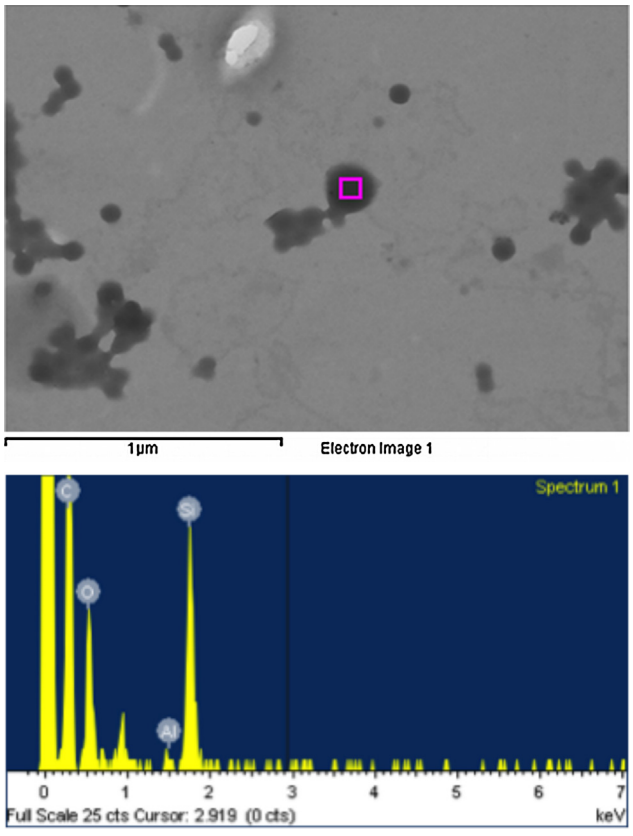

Fig. 5. EDX spectrum obtained from a bowl-structured particle. The presence of silicon indicates clay encapsulation by the polymer particle.

by polymer particles. It is worth saying that in the paper of Sun et al. (2004a,b) similar bowl-structured particles are also observed.

To explain the interaction between the clay and PMMA particles, it is possible to take Pickering emulsion phenomenon as an ideal model (Sedláková et al., 2009). In Pickering emulsions, solid colloidal particles with certain hydrophilicity stabilize water in oil or oil in water system (Betega de Paiva et al., 2008; Realinho et al., 2007). Since Nanofil SE3000 has been modified to interact with organic phases, it is expected that the hydrophobe surface present affinity with the monomer. It is important to remember that during sonication the clay was fragmented (and maybe exfoliated), leaving exposed, consequently, the unmodified clay surfaces to the polymerization medium. Therefore, the unmodified or poorly modified clay fractions interact preferable with the aqueous phase. Literature has shown that oil/water systems have been stabilized by the adsorption of clay platelets at the interface providing a physical barrier to coalescence (Pickering, 1907; Aveyard et al., 2003). In this sense, Negrete-Herrera et al. (2006a,b) reported the synthesis of styrene/butyl acrylate copolymers in the presence of organically modified nanometric laponite by emulsion polymerization. They observed that the latex particles (<100 nm) were covered by clay nanoplatelets, such observation was attributed to platelet functionalization, assumed on one face only due to exfoliation, which permitted the interfacial interaction with the polymer particles. Additionally, Voorn et al. (2006) reported the stabilization of inverse acrylamide emulsion polymerization merely by organically modified Cloisite20® (montmorillonite) platelets. They observed by electron microscopy the adsorption of the hydrophobic clay platelets at the surface of the poly(acryl amide) particles. Similarly, in the present situation a great concentration of PMMA particles are attached onto the clay surface, which indicated that such areas are chemically compatible with the polymer particles, suggesting that this kind of interaction is independent of phase dimensions.

Based on the above, it is possible to suggest that the bowl-structured particles were originated by the interaction of a small clay fragment and a polymer particle, where one side of the fragment is treated but not the other. This way, two possible scenarios may be considered: (a) when both sides are treated, the fragment is highly covered by polymer particles or (b) when both sides are untreated, the fragment is clean of polymer particles, as observed in Fig. 6(a and b).

3.3. Thermal and thermomechanical properties

To characterize thermal and mechanical behavior of the composites, differential scanning calorimetry (DSC) and dynamical mechanical analysis (DMA) were performed. Fig. 7 shows DSC traces of both the pure PMMA and the composites. As observed, in the composites the glass transition temperature (T_g) increased with respect to the pure PMMA (107 °C). Particularly, with 0.125 wt% and 0.5 wt% clay the T_g increased, respectively, 2 °C (109 °C) and 10 °C (117 °C). In the case of DMA, Fig. 8, increment of elastic modulus, E', in the glassy region with the addition of Nanofil SE3000 was observed. It is well known, however, that in this region molecular movements are highly restricted independently on the system morphology; therefore, filler effect is usually discrete. On the other hand, the increment of E', at the beginning of the rubbery plateau, is more significant as the good interfacial interaction polymer/filler is responsible for the restriction of the great molecular mobility of the polymeric matrix, characteristic of this regime. As seen, the increments on modulus with 0.125 wt% and 0.5 wt% clay were higher than with 1.0 wt% clay, just as the T_g determined by DSC. Complementarily, the analysis of loss modulus, E'', shown in Fig. 9, indicated a T_g of 100 °C for the pure PMMA; whereas T_gs of 103 °C, 110 °C, and 97 °C, respectively, for the composites with 0.125 wt%, 0.50 wt%, and 1.0 wt% clay, were determined. Certainly, even though there

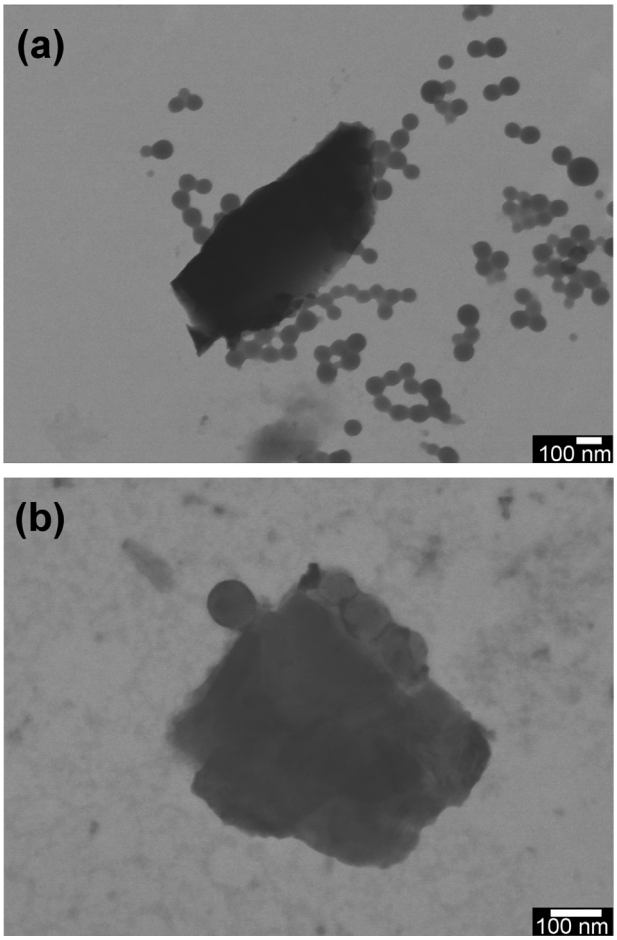

Fig. 6. Micrographs of clay fragments showing: (a) the surface of the fragment is clean of polymer particles indicating no affinity and (b) some polymer particles are adhered on a part of a clay fragment indicating surface affinity.

was slight difference between the T_g determined by DSC and DMA, the increments as a function of clay loading are in accordance.

As known, the addition of a solid filler to a polymer matrix increases T_g if strong interaction between both phases is present. In this case, the polymer chains are absorbed on the filler surface; consequently, the mobility of the chains closest to the surface is decreased. Therefore, near the filler surface the properties of the polymer may differ substantially from those observed in the bulk. Several models have been proposed to explain such interaction.

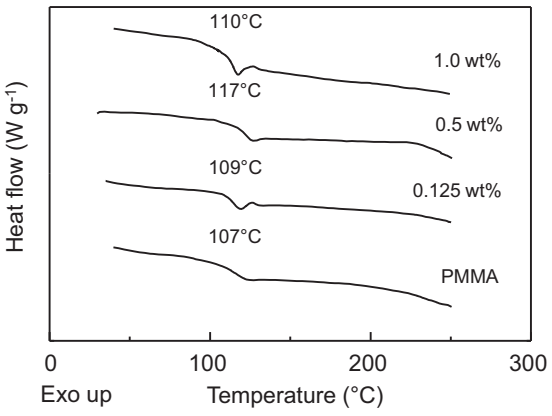

Fig. 7. DSC traces of the neat PMMA and the nanocomposites with 0.125 wt%, 0.5 wt%, or 1.0 wt% clay.

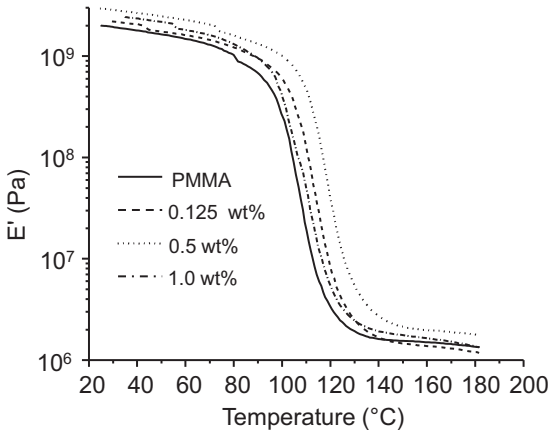

Fig. 8. Plots of elastic modulus (E') versus temperature, for the pure PMMA and the nanocomposites with 0.125 wt%, 0.5 wt%, or 1.0 wt% clay.

For instance, it has been reported that when the polymer chains present strong interfacial affinity with the filler surface, a region of strongly bound polymer chains is formed. This region, speculated to be within a few nanometers, has been called the "bound polymer layer" (Cousin and Smith, 1994). At higher lengths, it has been called the "interaction zone" (Tiarks et al., 2001). In this zone or region, the strongly packed polymer chains hinder chain segmental mobility, which occurs under standard conditions at the T_g. Consequently, more energy is required to allow the first thermal transitions, shifting T_g to a higher temperature.

Concerning the decrement both in T_g and in mechanical properties of the composite with the highest clay concentration, literature remarks such effect; for example, Ash et al. (2002a,b) reported T_g drops in the range 20 °C in nanometric alumina/PMMA composites. They proposed that this phenomenon was related to the lack of compatibility between the nanofiller and the polymer host; so that, chain mobility at the particle surface is very large but will drop off as the distance from the particle increases. Under these circumstances, the authors hypothesized that if the distance between filler nanoparticles is sufficiently small that bulk conditions are never reached, the nanocomposite will show a depression in T_g much like that observed in ultra-thin film research (Roth and Dutcher, 2005; Inoue et al., 2006; Pham et al., 2003). In a posterior report, Ash et al. (2002a,b) proved that by treating the alumina nanoparticles, to improve compatibility with the matrix, T_g depression was suppressed. In addition, Barrau et al. (2005) observed sudden T_g reductions close to the percolation concentration

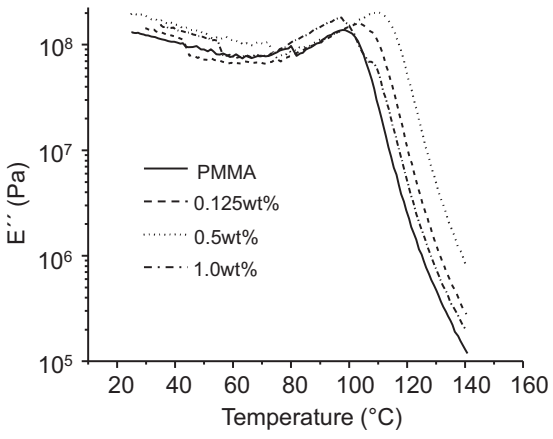

Fig. 9. Plots of loss modulus (E'') versus temperature, for the neat PMMA and the nanocomposites with 0.125 wt%, 0.5 wt%, or 1.0 wt% clay.

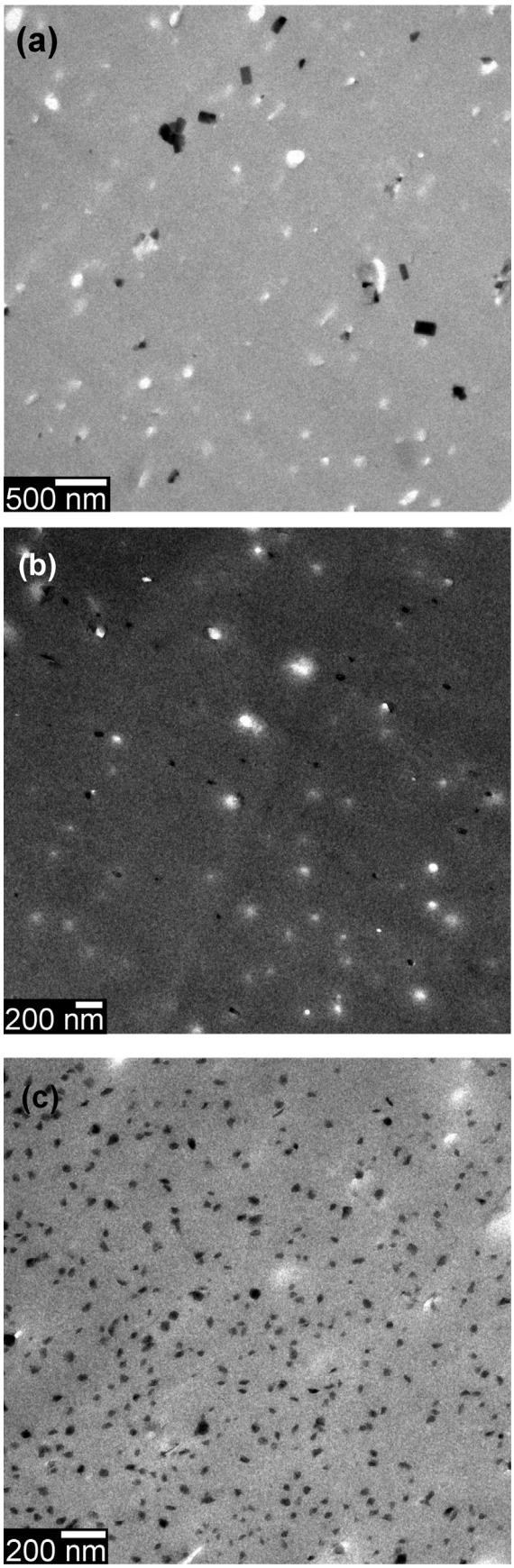

Fig. 10. Dispersion of the nanocomposites with (a) 0.125 wt%, (b) 0.5 wt%, or (c) 1.0 wt% clay. Both homogeneous clay dispersion and higher density of particles with clay content are evident.

in carbon nanotube/epoxy resin and polypyrrol/epoxy resin composites. They suggested that the T_g depression in the vicinity of the percolation concentration is interpreted as an increase of the mobility of the epoxy matrix chain segments. Just below this concentration, the conducting particles form many finite size clusters. In the percolation range, the free volume accessible to the molecular motions of epoxy chain segments is maximal exhibiting a plasticization-associated phenomenon. Under a similar viewpoint, Sun et al. (2004a,b) observed T_g reductions in nanofiller (silver, silica, alumminum, or carbon black)/epoxy resin composites. First, T_g was not affected by the micrometric counter parts of the nanofillers. However, because of the increased interfacial area in the nanocomposites (with respect to the micrometric composites) extra free volume at the resin–filler interface is created, consequently, assisted the large-scale segmental motion of the polymer, reducing T_g of the nanocomposites with increasing filler loading. Additionally, they emphasized the filler–matrix chemical interaction as a determining condition for T_g establishment. Other models to explain the interaction of polymers with nanoparticles can be consulted in literature (Sarvestani and Picu, 2004; Daoulas et al., 2005; Ramanathan et al., 2008; Sarvestani et al., 2008).

As seen, literature strongly emphasizes both filler–matrix compatibility and filler loading as responsible of T_g behavior; however, this important aspect in nanofiller–polymer composite science is controversial because of the inherent complexity of these materials. Taking inspiration from the literature, we have conducted an electron microscopy study to determine whether clay dispersion in the polymer host may help explain T_g drop at 1.0 wt% clay. Samples for microscopy were taken from the probes used for DMA characterization. Fig. 10(a–c) illustrates clay dispersion in the polymeric matrix; as shown in the three cases, the clay is dispersed in form of particles in the range of 100 nm and under. Besides, both homogeneous dispersion and higher density of particles as function of clay loading are evident. Accordingly, particle agglomeration seems not to be the apparent reason for the drop of thermal and mechanical properties at 1.0 wt% clay. However, the increased interfacial area with the content of clay is more than evident. Therefore, and in accordance with the cited literature, the increased filler–matrix interfacial area seems to be a determining condition for T_g depression. However, we would like to emphasize that the clay used in this study is a commercial material treated to enhance compatibility with the polymer matrix. Consequently, the combination of increased interfacial area and a weak chemical interaction between filler and polymer seem not to be the reason of T_g reduction; unless the method of synthesis has altered the clay surface treatment. Then, apparently, the interfacial area appears to be a more decisive factor than the chemical interaction. That is, with the increased proximity of the particles (as seen in Fig. 10c the distance among clay particles is in the submicrometric range) the possibility of the polymer chains to reach bulk conditions is restricted, consequently, the comparable effect of ultra-thin films is produced causing T_g dropping, as suggested by Ash et al. (2002a,b)

4. Conclusion

The applied methodology allowed the homogeneous incorporation of the clay in the polymer matrix. Changes in T_g and thermomechanical properties of the composites were observed as functions of clay loading. At the lower clay contents (0.125 wt% and 0.5 wt%) both properties increased; whereas at the highest load (1.0 wt%) both of them dropped. There is controversy concerning the explanation of such a behavior in nanofiller–polymer composites, where aspects like interfacial area and nanofiller–polymer chemical interaction seem to be determining. However, a universal explanation of this phenomenon is still under study since the different nature of the nanofiller and the matrix and their possible

combinations make this task a great challenge. Finally, we can conclude that, at least in the present case, the increased interfacial area nanofiller–matrix played the most important role in determining both glass transition and thermomechanical properties, in a similar way as in the polymeric ultra-thin films.

Acknowledgements

We wish to thank the National Council for Science and Technology of Mexico (CONACYT) for the Grant awarded to Karla I. García-Castillo. We also wish to thank to the Laboratorio Nacional de Nanotecnología, and to Mónica Mendoza, Daniel Lardizabal, Wilber Antunez, and Enrique Diazbarriga for their helpful collaboration during this research.

References

Ash, B.J., Rogers, D.F., Wiegand, C.J., Schadler, L.S., Siegel, R.W., Benicewicz, B.C., Apple, T., 2002a. Mechanical properties of Al_2O_3/polymethylmethacrylate nanocomposites. Polymer Composites 23, 1014–1025.

Ash, B.J., Schadler, L.S., Siegel, R.W., 2002b. Glass transition behavior of alumina/polymethylmethacrylate nanocomposites. Materials Letters 55, 83–87.

Aveyard, R., Binks, B.P., Clint, J.H., 2003. Emulsions stabilised solely by colloidal particles. Advances in Colloid Interface Science 100–102, 503–546.

Barrau, S., Demont, P., Maraval, C., Bernes, A., Lacabanne, C., 2005. Glass transition temperature depression at the percolation threshold in carbon nanotube–epoxy resin and polypyrrole–epoxy resin composites. Macromolecular Rapid Communications 26, 390–394.

Betega de Paiva, L., Morales, A.R., Valenzuela Díaz, F.R., 2008. Organoclays: properties, preparation and applications. Applied Clay Science 42, 8–24.

Bouanani, F., Bendedouch, D., Hemery, P., Bounaceur, B., 2008. Encapsulation of montmorillonite in nanoparticles by miniemulsion polymerization. Colloids and Surfaces A – Physicochemical and Engineering Aspects 317, 751–755.

Cousin, P., Smith, P., 1994. Dynamic mechanical properties of sulfonated polystyrene/alumina composites. Journal of Polymer Science 32, 459–468.

Daoulas, K.C., Harmandaris, V.A., Mavrantzas, V.G., 2005. Detailed atomistic simulation of a polymer melt/solid interface: structure, density, and conformation of a thin film of polyethylene melt adsorbed on graphite. Macromolecules 38, 5780–5795.

Hao, L., Yunzhao, Y., Yukun, Y., 2005. Synthesis of exfoliated polystyrene/montmorillonite nanocomposite by emulsion polymerization using a zwitterion as the clay modifier. European Polymer Journal 41, 2016–2022.

Inoue, R., Kanaya, T., Miyazaki, T., Nishida, K., Tsukushi, I., Shibata, K., 2006. Glass transition and thermal expansivity of polystyrene thin films. Materials Science and Engineering A 442, 367–370.

Lai, M.C., Chang, K.C., Yeh, J.M., Liou, S.J., Hsieh, M.F., Chang, H.S., 2007. Advanced environmentaly friendly anticorrosive materials prepared from water-based polyacrylate/Na+-MMT clay nanocomposite latex. European Polymer Journal 43, 4219–4228.

Lu, C., Mai, Y.-W., 2005. Influence of aspect ratio on barrier properties of polymer–clay nanocomposites. Physical Review Letters 95, 088303.

Mirzataheri, M., Mahdavian, A.R., Atai, M., 2009. Nanocomposite particles with core–shell morphology IV: an efficient approach to the encapsulation of Cloisite 30B by poly (styrene-co-butyl acrylate) and preparation of its nanocomposite latex via miniemulsion polymerization. Colloid and Polymer Science 287, 725–732.

Negrete-Herrera, N., Putaux, J.-L., Bourgeat-Lami, E., 2006a. Synthesis of polymer/laponite nanocomposite latex particles via emulsion polymerization using silylated and cation-exchanged laponite clay platelets. Progress in Solid State Chemistry 34, 121–137.

Negrete-Herrera, N., Putaux, J.-L., David, L., Bourgeat-Lami, E., 2006b. Polymer/laponite composite colloids through emulsion polymerization: influence of the clay modification level on particle morphology. Macromolecules 39, 9177–9184.

Noh, M.W., Lee, D.C., 1999. Synthesis and characterization of PS-clay nanocomposite by emulsion polymerization. Polymer Bulletin 42, 619–626.

Pham, J.Q., Mitchell, C.A., Bahr, J.L., Tour, J.M., Krishanamoorti, R., Green, P.F., 2003. Glass transition of polymer/single-walled carbon nanotube composite films. Journal of Polymer Science Part B: Polymer Physics 41, 3339–3345.

Pickering, S.U., 1907. Emulsions. Journal of the Chemical Society 91, 2001–2021.

Ramanathan, T., Abdala, A.A., Stankovich, S., Dikin, D.A., Herrera-Alonso, M., Piner, R.D., Adamson, D.H., Schniepp, H.C., Chen, X., Ruoff, R.S., Nguyen, S.T., Aksay, I.A., Prudĩhomme, R.K., Brinson, L.C., 2008. Functionalized graphene sheets for polymer nanocomposites. Nature Nanotechnology 3, 327–331.

Realinho, V., Antunes, M., Arencón, D., Gordillo, A., Martínez, A.B., Velasco, J.I., 2007. Tenacidad a la fractura de nanocompuestos de PMMA con montmorillonita: influencia de la orientación inducida en el procesado. Anales de la Mecánica de Fractura 1, 353–358.

Roth, C.B., Dutcher, J.R., 2005. Glass transition and chain mobility in thin polymer films. Journal of Electroanalytical Chemistry 584, 13–22.

Sarvestani, A.S., Picu, C.R., 2004. Network model for the viscoelastic behavior of polymer nanocomposites. Polymer 45, 7779–7790.

Sarvestani, A.S., He, X., Jabbari, E., 2008. The role of filler-matrix interaction on viscoelastic response of biomimetic nanocomposite hydrogels. Journal of Nanomaterials (ID 126803).

Sedláková, Z., Plesštil, J., Baldrian, J., Šlouf, M., Holub, P., 2009. Polymer–clay nanocomposites prepared via in situ emulsion polymerization. Polymer Bulletin 63, 365–384.

Sun, Q., Deng, Y., Wang, Z.L., 2004a. Synthesis and characterization of polystyrene-encapsulated laponite composites via miniemulsion polymerization. Macromolecular Materials and Engineering 289, 288–295.

Sun, Y.Y., Zhang, Z.Q., Moon, K.S., Wong, C.P., 2004b. Glass transition and relaxation behavior of epoxy nanocomposites. Journal of Polymer Science Part B: Polymer Physics 42, 3849–3858.

Tiarks, F., Landfester, K., Antonietti, M., 2001. Encapsulation of carbon black by miniemulsion polymerizatio. Macromolecular Chemistry and Physics 202, 51–60.

Tong, Z., Deng, Y., 2007. Synthesis of polystyrene encapsulated nanosaponite composite latex via miniemulsion polymerization. Polymer 48, 4337–4343.

Voorn, D.J., Ming, W., van Herk, A.M., 2006. Polymer–clay nanocomposite latex particles by inverse Pickering emulsion polymerization stabilized with hydrophobic montmorillonite platelets. Macromolecules 39, 2137–2143.

Xu, M., Choi, Y.S., Kim, Y.K., Wang, K.H., Chung, I.J., 2003. Synthesis and characterization of exfoliated poly(styrene-co-methyl methacrylate)/clay nanocomposites via emulsion polymerization. Polymer 44, 6387–6395.

Xu, Y., Brittain, W.J., Vaia, R.A., Price, G., 2006. Improving the physical properties of PEA/PMMA blends by the uniform dispersion of clay platelets. Polymer 47, 4564–4570.

Yeh, J.-M., Liou, S.-J., Lai, M.-C., Chang, Y.-W., Huang, C.-Y., Chen, C.-P., Jaw, J.-H., Tsai, T.-Y., Yu, Y.-H., 2004. Comparative studies of the properties of poly(methyl methacrylate)–clay nanocomposite materials prepared by in situ emulsion polymerization and solution dispersion. Journal of Applied Polymer Science 94, 1936–1946.